Title	Vortex dynamics in twinned superconductors
Author(s)	Zhu, BY; Dong, J; Xing, DY; Wang, ZD
Citation	Physical Review B - Condensed Matter And Materials Physics, 1998, v. 57 n. 9, p. 5075-5078
Issued Date	1998
URL	http://hdl.handle.net/10722/43220
Rights	Physical Review B (Condensed Matter). Copyright © American Physical Society.

Vortex dynamics in twinned superconductors

B. Y. Zhu, Jinming Dong, and D. Y. Xing
National Laboratory of Solid State Microstructures, and Department of Physics, Nanjing University, Nanjing 210093, People's Republic of China

Z. D. Wang
Department of Physics, University of Hong Kong, Hong Kong, People's Republic of China

(Received 22 September 1997)

We numerically solve the overdamped equation of vortex motion in a twin-boundary (TB) superconductor, in which the applied Lorentz force F_L, the pinning forces due to TB's and point defects, and the intervortex interacting force are taken into account. Our simulations show that TB's act as easy flow channels for the vortex motion parallel to the TB's and obstructive barriers for that normal to the TB's. Due to the barrier effect, the transverse velocity of vortices increases with F_L, but if F_L is strong enough, the vortices can cross through the TB's so that the transverse velocity vs F_L curve exhibits peak behavior. [S0163-1829(98)01010-8]

In recent years the vortex dynamics in the mixed state of high-T_c superconductors has been a topic of great interest,[1] and vortex pinning plays an important role in determining the vortex structures and its dynamics. Various defect structures, including oxygen-vacancy clusters, growth flux inclusions, second phases, and twin boundaries (TB's), were suggested to act as pinning centers of vortex motion in cuprate superconductors. Among them TB's may be the most important anisotropic pinning defects in the orthorhombic compound $YBa_2Cu_3O_{7-x}$ (YBCO).[2] The TB's have been studied by numerous experimental techniques.[2–18] It is found[2,3] that the strength of the TB pinning is highly dependent on the orientation of the magnetic field with the twin planes. The TB planes are strong pinning centers in the flux-flow regime when they are aligned parallel to the magnetic field,[2] leading to anomalous behavior of the vortex motion in the vicinity of TB's. There existed controversy concerning the effect of TB's.[4–7] The magneto-optical measurements by Duran *et al.*[4] indicate that the TB's act as easy-flow channels for longitudinal vortex motion. By using the same techniques, Vlasko-Vlasov *et al.*[5] showed that the TB's are strong barriers for transverse vortex motion, resulting in a buildup of flux on the side of the TB facing the motion and a corresponding shadow on the opposite side. Based on the magnetic hysteresis measurements, Oussena *et al.*[8] found that TB's can act as channels for vortex motion, but channeling of vortices along the TB is only effective when the pinning in the untwinned regions between the twin planes becomes stronger. Recent results[6,7] have shown that there is an angular dependence; i.e., a TB may act as either an easy-flow channel or a barrier, depending on the relative direction of flux motion with respect to the TB. Although many studies have addressed the TB effects on the vortex dynamics in the mixed state, this issue is still far from being solved.

Very recently, Groth *et al.*[15] performed a numerical simulation of flux-gradient-driven vortices in twinned superconductors with a large amount of point pinning defects. They took into account vortex-vortex, vortex-pin, and vortex-twin interactions to investigate how these vortices travel through the sample in the presence of both TB and point defect pinning. In their simulation the vortices are driven by the flux gradient and the vortex-vortex interaction. Since no applied current was considered there, the Lorentz force acting on the vortices is absent in the overdamped motion equation, so that such a simulation fails to account for the experimental results of vortex transport measurements on twinned superconductors. As a result, it is highly desirable to extend this simulation to the case with an applied current so as to study the TB effects on the vortex motion driven by the Lorentz force.

In this paper, by taking the TB's as attractive wells, we study how the vortices travel in a twinned sample with increasing the applied current. Particular attention is paid to the angular dependence of the average moving velocity of vortices. The simulation results show that the TB's can act as either easy-flow channels or obstructive barriers for the vortex motion, depending strongly on the orientation of the applied currents with respect to the TB's. If the applied Lorentz force is strong enough, the vortices can escape from the TB traps and cross through them.

Our simulation geometry is that of an infinite slab of superconductor under a magnetic field perpendicular to the slab surface and parallel to the TB planes. Following the model of Ref. 15, we treat the vortices as stiff pillars, so that we need to model only a two-dimensional (2D) slice of the 3D slab. In the present dynamic simulation, we take into account a 2D rectangular system (x-y plane) with periodic boundary conditions for both TB's and point defects. It is necessary to vary the angle between the applied current and the TB lines in the 2D slice to investigate the angular dependence of the vortex motion. This can be achieved either by fixing the 2D slice and changing the orientation of the applied current, or by fixing the latter and revolving the slice on the z axis. Both of them should yield the same simulated result. In the present simulation, we always take the x axis along the orientation of the applied currents so that the Lorentz force has only a y component. To apply readily the periodic boundary condition to the 2D slice, we assume the TB lines to be parallel to each other and to have the same spacing $d_{\rm TB}$.

Consider the Lorentz force $\mathbf{F}_L$, the intervortex interacting force $\mathbf{F}_{vv}(\mathbf{r}_i)$, the pinning forces $\mathbf{F}_{\rm pin}(\mathbf{r}_i)$ generated by ran-

0163-1829/98/57(9)/5075(4)/$15.00

domly distributed point pinning centers and $\mathbf{F}_{\rm pin}^{\rm TB}(\mathbf{r}_i)$ by periodically distributed TB's, and the Brownian force $\mathbf{F}_{\rm th}$ due to the Gaussian thermal noise.[19] The overdamped equation for the ith vortex moving with velocity $\mathbf{v}_i$ can be written as

$$\eta\mathbf{v}_i=\mathbf{F}_L+\mathbf{F}_{vv}(\mathbf{r}_i)+\mathbf{F}_{\rm pin}(\mathbf{r}_i)+\mathbf{F}_{\rm pin}^{\rm TB}(\mathbf{r}_i)+\mathbf{F}_{\rm th}, \qquad (1)$$

where η is the viscous coefficient (we take $\eta=1$) and $\mathbf{r}_i$ denotes the location of the ith vortex. The Lorentz force applied to the vortex is given by $\mathbf{F}_L=\mathbf{J}\times\mathbf{\Phi}_0$ where $\mathbf{J}$ is the applied current and $\mathbf{\Phi}_0$ is the flux quantum. The repulsive intervortex interaction employed here has a logarithmic form[20] and the expression for $\mathbf{F}_{vv}$ is given by

$$\mathbf{F}_{vv}(\mathbf{r}_i)=F_{vv0}f_0\sum_{j\neq i}^{N_v}\frac{(\mathbf{r}_i-\mathbf{r}_j)/R_{\rm vor}}{|(\mathbf{r}_i-\mathbf{r}_j)/R_{\rm vor}|^2}. \qquad (2)$$

Here $F_{vv0}f_0$ denotes the intensity of the intervortex interacting force, with $f_0=\Phi_0^2/(8\pi^2\lambda^3)$ as the unit of force in our simulations.[15] N_v is the number of vortices in the slice, and $R_{\rm vor}$ is the decay length of this long-range repulsive force, which corresponds to the superconducting penetration depth λ. The thermal fluctuation force $\mathbf{F}_{\rm th}$ is taken to be the Gaussian-type form given by Ref. 19. Since we focus our attention on a small low temperature regime, $\mathbf{F}_{\rm th}$ is taken to be independent of temperature in the present work.

The point pinning centers are modeled by Gaussian potential wells with a decay length $R_{\rm pin}$,[19] and so the pinning force acting on the vortex at $\mathbf{r}_i$ is given by

$$\mathbf{F}_{\rm pin}(\mathbf{r}_i)=-F_{p0}f_0\sum_{k}^{N_p}\frac{\mathbf{r}_i-\mathbf{R}_k}{R_{\rm pin}}\exp\left(-\left|\frac{\mathbf{r}_i-\mathbf{R}_k}{R_{\rm pin}}\right|^2\right). \qquad (3)$$

Here $F_{p0}f_0>0$ denotes the intensity of the individual pinning force, N_p is the number of the point pinning centers, and $\mathbf{R}_k$ stands for the location of the kth point pinning center. We model the attractive TB well as a parabolic channel with a width $2R_{\rm pin}^{\rm TB}$. The attractive pinning force on the vortex at $\mathbf{r_i}$ due to the lth TB can be written as[21]

$$\mathbf{F}_{\rm pin}^{\rm TB}(\mathbf{r}_i)=-F_{p0}^{\rm TB}f_0\sum_{l}^{N_{\rm TB}}t_{il}(1-t_{il}^2)\Theta(1-|t_{il}|)\hat{\mathbf{n}}, \qquad (4)$$

where $t_{il}=d_{il}^{\rm TB}/R_{\rm pin}^{\rm TB}$ with $d_{il}^{\rm TB}$ the perpendicular distance between the ith vortex and the lth TB. $F_{p0}^{\rm TB}f_0>0$ denotes the intensity of the TB pinning force and $F_{p0}^{\rm TB}$ is an adjust parameter to vary the intensity. $N_{\rm TB}$ stands for the number of the TB's in the slice, $\Theta(x)$ is a unit step function, and $\hat{\mathbf{n}}$ presents the unit vector normal to the TB line.

Many parameters can be varied, making the systematic study of this problem quite complex. Here we choose to vary four critical variables: the angle θ between the TB and the Lorentz force $\mathbf{F}_L$, the pinning force $F_{p0}^{\rm TB}$ due to TB's, and the ratio F_{Ly}/f_0 with F_{Ly} the Lorentz force. All the other parameters are fixed as follows, among which forces are measured in units of f_0 and lengths in units of λ. First, we take $F_{vv0}=0.05$, $F_{p0}=0.2$, and the corresponding thermal noise force $F_{\rm th0}=0.01$. Second, $R_{\rm pin}^{\rm TB}=2R_{\rm pin}=0.1$, and $R_{\rm vor}=1$, the cut length of the long-range repulsive force between vortices being $4R_{\rm vor}$. Third, we take $d_{\rm TB}=2$, and the point defect density and vortex density to be $70/\lambda^2$ and $3.5/\lambda^2$, respectively. The actual sample used in our simulations is $10\times12\lambda^2$ so that $N_v=420$ and $N_p=8400$. If we take $\lambda=1400$ Å, a typical value observed on YBCO samples, the spacing $d_{\rm TB}$ of TB's is equal to 2800 Å, which is a reasonable value close to the experimental data.[16] Finally, the applied magnetic field is fixed as $3.5\Phi_0/\lambda^2$, which is about $0.37T$. With these parameters, we employ a molecular dynamical simulation[22] to numerically solve Eqs. (1)–(4). The data of the curves will be obtained by averaging total 40 000 run steps, discarding the first 10 000 runs to assure achievement of a steady state. The error in calculation is estimated less than 1%.

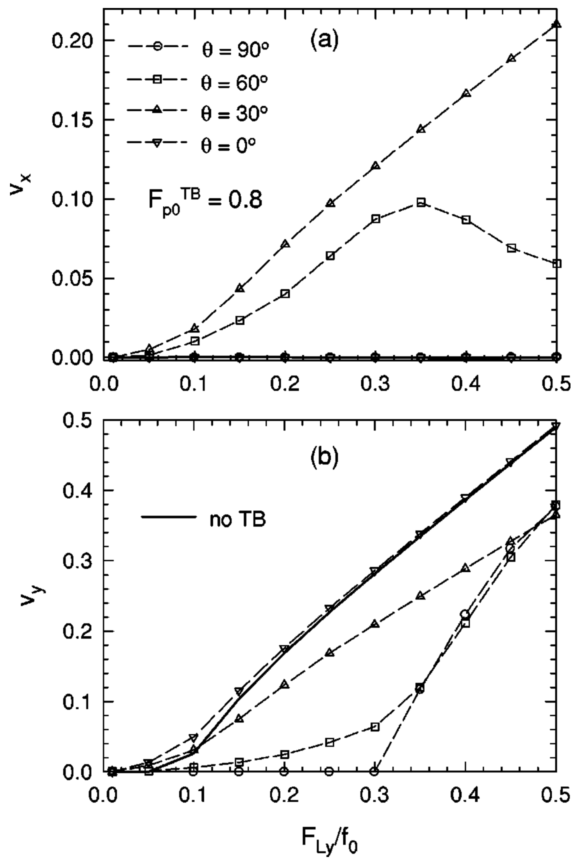

FIG. 1. The transverse (a) and the longitudinal (b) components of the average vortex velocity in a TB system as functions of the applied Lorentz force $\mathbf{F}_{Ly}$ for several angles between the Lorentz force and the TB's. Here $F_{p0}^{\rm TB}=0.8$ and $F_{p0}=0.2$ are fixed.

We plot the average moving velocities of vortices vs the Lorentz force in Fig. 1 to show the angular dependence of vortex motion in the TB pinning system. The intensity of the attractive TB forces is fixed as $F_{p0}^{\rm TB}=0.8$. From Fig. 1, we can see that with increasing the driving Lorentz force, the average velocities v_x and v_y of vortices show an obvious angular dependence. The longitudinal velocity v_y of vortices increases monotonously with F_{Ly}, as shown in Fig. 1(b), but the transverse v_x perpendicular to $\mathbf{F}_L$ shows a quite different behavior in Fig. 1(a). For TB's right parallel or perpendicular to $\mathbf{F}_L$, corresponding to $\theta=0°$ or $\theta=90°$, there is no transverse motion of vortices, i.e., $v_x=0$. For ease of comparison, the v_y vs F_{Ly} behavior in the absence of a TB is plotted as the solid line in Fig. 1(b). We see that v_y at $\theta=0$ is greater than that in the absence of a TB, in particular in the low F_{Ly}

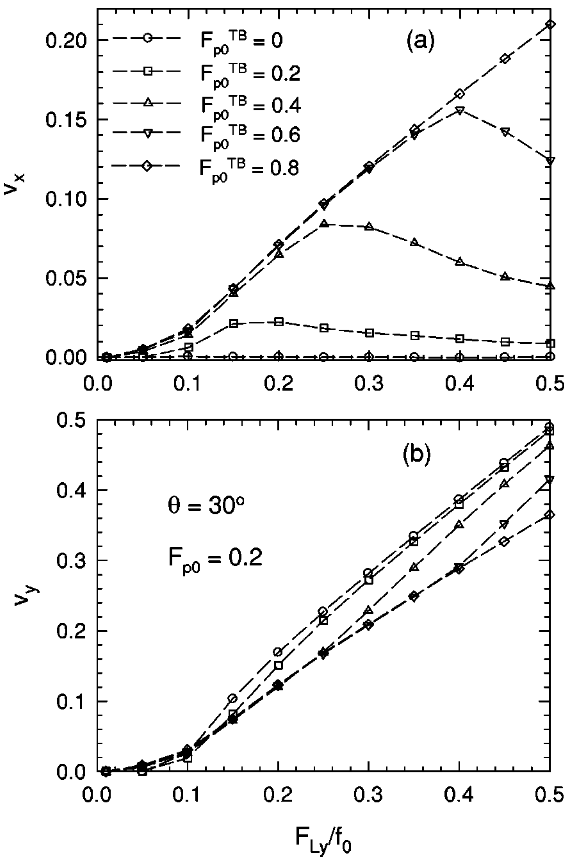

FIG. 2. The transverse (a) and the longitudinal (b) components of the average vortex velocity at $\theta=30°$ as functions of the applied Lorentz force for different F_{p0}^{TB}.

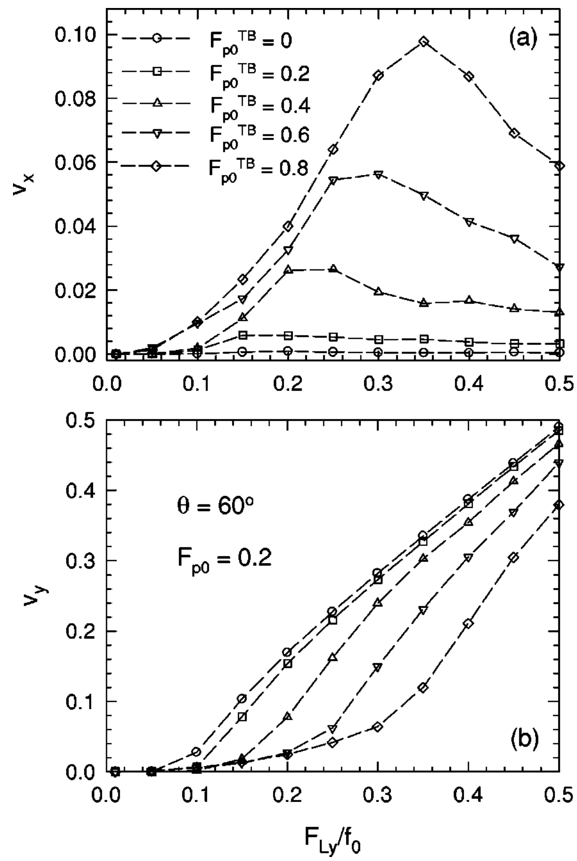

FIG. 3. The transverse (a) and the longitudinal (b) components of the average vortex velocity at $\theta=60°$ as functions of the applied Lorentz force for different F_{p0}^{TB}.

region, while the v_y vs F_{Ly} curve at $\theta=90°$ is well below the solid line; e.g., a nonzero v_y does not appear until $F_{Ly}/f_0=0.30$. It follows that the TB's can act as either easy-flow channels for vortex motion when the TB lines are parallel to $\mathbf{F}_L$ ($\theta=0°$), or barriers when the TB lines are perpendicular to $\mathbf{F}_L$ ($\theta=90°$). For $0<\theta<90°$, the transverse component v_x of vortex motion appears. With increasing F_{Ly}, at $\theta=60°$ v_x first increases and then decreases, exhibiting a peak at $F_{Ly}/f_0\simeq0.35$, while at $\theta=30°$, v_x increases monotonously. Such an interesting behavior can be understood by the following argument. In this simulation, $F_{p0}^{\mathrm{TB}}/F_{p0}=4$ has been taken, implying that the pinning effect of TB's is stronger than that of the point pinning centers, so that the pining effect of the vortices comes mainly from the TB potentials. The TB's act as barriers for the vortex motion component perpendicular to the TB's and as an easy-flow channel for that parallel to the TB's, being favorable for the vortices moving along the TB's. It is this effect that leads to the appearance of v_x, v_x increasing with F_{Ly}. However, when the perpendicular component of F_{Ly} becomes large enough [$F_{Ly}\sin\theta/f_0\geqslant0.30$, the threshold value of F_{Ly} depending on the angle θ (Ref. 23)], a part of vortices can escape from the TB channel and cross through the TB barrier, making v_x decrease with increasing $\mathbf{F}_L$. According to the above argument, the threshold values of F_{Ly}/f_0 are about 0.35 for $\theta=60°$ and 0.60 for $\theta=30°$, respectively. This can explain why the v_x vs F_{Ly} curve has a peak structure at $F_{Ly}\simeq0.35$ for the former and varies monotonously in the range of $F_{Ly}/f_0\leqslant0.50$ for the latter.

To clearly see this point, we present v_x and v_y as functions of the applied Lorentz force for different F_{p0}^{TB} in Fig. 2 ($\theta=30°$) and Fig. 3 ($\theta=60°$). For $F_{p0}^{\mathrm{TB}}=0$, there is nearly no transverse motion of vortices ($v_x\simeq0$) at both $\theta=30°$ and 60°. In this case, there exists no obstructive barrier for the transverse motion of vortices, but there remains a little of the channel effect on the longitudinal motion since the point pinning defects are assumed absent within the TB regions. With the increase of F_{p0}^{TB}, v_x increases and v_y decreases, indicating that both the easy-flow channel and obstructive barrier effects on the vortex motion are gradually enhanced. Such effects are more evident at $\theta=60°$ than that at $\theta=30°$. This may stem from the fact that in the former the perpendicular component of the Lorentz force, $F_{Ly}\sin\theta$, is larger. The threshold value of F_{Ly}, at which v_x reaches its maximum, is determined by the pinning strength of the TB's, as shown in Figs. 2(a) and 3(a). One sees that with increasing F_{p0}^{TB}, the threshold value increases and the v_x vs F_{Ly} peak shifts towards the right. For the same F_{p0}^{TB}, the threshold value of F_{Ly} at $\theta=30°$ is usually larger than that at $\theta=60°$, as has been discussed above. At present there is no direct experiment to study the effect of the TB pinning strength on the vortex motion. However, by using the heavy-ion irradiation technique, one can vary the intensity of the point pinning potential in the samples[24] so as to adjust the ratio

$F_{p0}^{\mathrm{TB}}/F_{p0}$. It is expected that the interesting behavior of the vortex motion for different F_{p0}^{TB} could be observed in future experiments.

In the present simulations some approximations have been made. First, the temperature effect is implicitly included only by varying the ratio $F_{p0}^{\mathrm{TB}}/F_{p0}$. The ratio is expected to be a function of temperature T, which is small for low T and larger for higher T. By varying this ratio, we can mimic some of the effects due to temperature. However, we have not taken into account the temperature dependence of the thermal noise force $\mathbf{F}_{\mathrm{th}}$. Second, in Eq. (1) we have used the same viscous coefficient within the TB regions and in the untwinned regions, as done in Ref. 15. The viscous coefficient η in the TB regions may differ from that in the point pinning regions. However, this difference would not change the qualitative conclusion obtained in this paper. Finally, the present TB potential is assumed to be an attractive pinning well, as same as those of point pinning centers. We have also studied a repulsive TB model by taking F_{p0}^{TB} to have the opposite sign. It is found that the two components of the average vortex velocity are almost the same for both the attractive and repulsive TB models if the same amplitude $|F_{p0}^{\mathrm{TB}}|$ is used. The main difference is that the easy-flow channels are within the TB's in the attractive TB model, while they are on the side of the TB's facing the vortex motion in the repulsive TB model.

In summary, the present molecular dynamical simulations show that for a TB pinning system, the behavior of vortex motion depends strongly on the orientation of TB's with respect to the applied current. The TB's are found to act as easy-flow channels for vortex motion parallel to the TB's and obstructive barriers for that normal to the TB's. The strength of the TB pinning potentials plays an important role in determining the transverse motion of vortices. When the Lorentz force is strong enough as compared with the TB pinning force, the vortices can cross through the TB barriers, giving rise to a decrease in the transverse velocity of vortices and a rapid increase in their longitudinal velocity.

This work was supported by the National Center for Research and Development on Superconductivity of China.

[1] G. Blatter *et al.*, Rev. Mod. Phys. **66**, 1125 (1994).
[2] W. K. Kwok *et al.*, Phys. Rev. Lett. **64**, 966 (1990).
[3] S. Fleshler *et al.*, Phys. Rev. B **47**, 14 448 (1993).
[4] C. A. Duran *et al.*, Nature (London) **357**, 474 (1992).
[5] V. K. Vlasko-Vlasov *et al.*, Phys. Rev. Lett. **72**, 3246 (1994).
[6] C. A. Duran *et al.*, Phys. Rev. Lett. **74**, 3712 (1995).
[7] U. Welp *et al.*, Phys. Rev. Lett. **74**, 3713 (1995).
[8] M. Oussena *et al.*, Phys. Rev. B **51**, 1389 (1995); Phys. Rev. Lett. **76**, 2559 (1996).
[9] A. A. Zhukov *et al.*, Phys. Rev. B **52**, R9871 (1995).
[10] D. Lopez *et al.*, Phys. Rev. B **53**, R8895 (1996).
[11] E. F. Righi *et al.*, Phys. Rev. B **55**, 5663 (1997).
[12] R. Hiergeist and R. Hergt, Phys. Rev. B **55**, 3258 (1997).
[13] R. J. Wijngaarden *et al.*, Phys. Rev. B **55**, 3268 (1997).
[14] H. Safar *et al.*, Appl. Phys. Lett. **68**, 1853 (1996).
[15] J. Groth *et al.*, Phys. Rev. Lett. **77**, 3625 (1996).
[16] W. K. Kwok *et al.*, Phys. Rev. Lett. **76**, 4596 (1996).
[17] L. J. Swartzendruber *et al.*, Phys. Rev. Lett. **64**, 483 (1990).
[18] D. Lopez *et al.*, Phys. Rev. Lett. **76**, 4034 (1996).
[19] Z. D. Wang *et al.*, Phys. Rev. B **51**, 6119 (1995); B. Y. Zhu, Physica C **276**, 309 (1997).
[20] K. Yates, D. J. Newman, and P. A. J. de Groot, Phys. Rev. B **52**, R13 149 (1995); Physica C **241**, 111 (1995).
[21] K. Moon, R. T. Scalettar, and G. T. Zimanyi, Phys. Rev. Lett. **77**, 2778 (1996).
[22] M. C. Faleski, M. C. Marchetti, and A. A. Middleton, Phys. Rev. B **54**, 12 427 (1996).
[23] The threshold value of F_{Ly} depends also on the magnitude of F_{p0}^{TB} and the vortex density.
[24] A. V. Samoilov *et al.*, Phys. Rev. Lett. **74**, 2351 (1995).